

Roman Alejandro Werner^{1*}
Ronny Takacs¹
Patrick Morsch²
Dominik Ulrich Geier¹
Hermann Nirschl²
Thomas Becker¹

Jet Cleaning of Filter Cloths Used in Solid-Liquid Separation: A High-Speed Video Evaluation

Cleaning avoids cross-contamination and sustains production safety and efficiency. While there have been discoveries for technical surfaces, data on activities for filter cloth are still in the early stages. In the food industry, there is a lack of knowledge and innovative ideas on how to clean cloths efficiently. This study combined high-speed recordings with cleaning experiments. Cleaning of eleven filters was captured, enabling time-resolved analysis of the cleaning degree, the cleaning homogeneity, and insights into the mechanisms. The findings divide cloth cleaning into three phases, each significantly influenced by the properties of the cloth. Exemplarily, close-mesh cloths have smoother surfaces that facilitate cleaning. Coarse structures with flow channels on the cloth surface can complicate cleaning.

Keywords: Cleaning control, Filter cloth cleaning, Filter press, High-speed video analysis, Nozzle cleaning

Received: October 02, 2022; *revised:* January 08, 2023; *accepted:* January 11, 2023

DOI: 10.1002/ceat.202200468

 This is an open access article under the terms of the Creative Commons Attribution-NonCommercial License, which permits use, distribution and reproduction in any medium, provided the original work is properly cited and is not used for commercial purposes.



Supporting Information
available online

1 Introduction

Cleaning is one of the most crucial unit operations in the food industry. As defined by the German DIN 10516 [1], cleaning removes all (visible) contamination from any surface when using a suitable cleaning utensil. Cleaning success is well known to be dependent on the temperature, the chemical agents, mechanical effects, and the time [2]. Furthermore, publications in recent years have demonstrated that the targeted contamination and the surface characteristics have a high cleaning impact, as well [3]. Cleanability in this context refers to how easily a surface can be cleared of adhering contamination in terms of time, fluid consumption, and the thoroughness of the cleaning.

Increasing cleaning efficiency is essential for economic and ecological reasons [2, 4, 5]. While cleaning vessels, equipment, and technical surfaces were researched extensively, other items, such as filter media, have received little attention. Exemplary media are woven filter cloths applied in filter systems, e.g., presses. These fabrics enable solid-fluid separation in food production, e.g., mash filtration in breweries. They form the barrier that keeps the retentate in place while allowing the filtrate to pass through. Filter cloths are textiles with warp and weft threads interwoven to distinct weave patterns [6]. The threads vary in diameter and can be monofil (one single thread) or multifil (various threads twisted into one). These cloth characteristics determine the resulting mesh sizes. Such cloth parameters can be summed up to the term filter geometry, which represents the complexity of the cloth and influences the its cleanability.

According to the European Hygienic Engineering & Design Group (EHEDG) [7], the roughness of a surface plays a vital role in its cleanability. Although Mauermann et al. [8] identified more influence of the surface energy and less of rougher stainless-steel surfaces, a more significant roughness influence can be assumed for cloths due to an excessively complex surface. Especially here, a significant backlog demand in cleaning exists. While the actual filtration processes are well understood, the regeneration of filters still adheres to rigid and exaggerated concepts. Although there are partly automated concepts, most of the cleaning depends on the operator's experience and never considers the degree of contamination present. Thus, exaggerated cleaning is used to achieve a safe status at the cost of economic and ecological aspects. There is a lack of optimization and necessary approaches for enabling innovative, fully automated, demand-oriented, or digitalized methods. Finally, the corresponding manufacturing recommendations for hygienic design can still be improved [9].

¹Roman Alejandro Werner  <https://orcid.org/0000-0002-6911-2591>, Ronny Takacs  <https://orcid.org/0000-0001-7629-6491>, Dominik Ulrich Geier, Prof. Dr. Thomas Becker (roman.werner@tum.de)

Technical University of Munich (TUM), TUM School of Life Sciences, Chair of Brewing and Beverage Technology, Weihenstephaner Steig 20, 85354 Freising, Germany.

²Dr. Patrick Morsch, Prof. Dr. Hermann Nirschl Karlsruhe Institute of Technology (KIT), Institute for Mechanical Process Engineering and Mechanics – Process Machines, Strasse am Forum 8, 76131 Karlsruhe, Germany.

Previous studies looked at the particle-based cleanability of filter cloths and cleaning efficiency test procedures [10–12]. Necessary cleaning parameters of wash jet cleaning for model and food-related contaminations were studied by Morsch et al. [13, 14]. Other publications focused on alternative cleaning procedures like pulsatile jet cleaning [15–18]. These publications paved the way for a first understanding and optimization of cloth cleaning and the development of new concepts. However, a thorough examination of the critical cleaning mechanisms and the influence of different cloth properties is lacking, although being especially crucial in food applications. For instance, in previous studies, only the status before and after the cleaning procedure was observed, which leaves out the critical steps of a wash jet affecting the cloth. Most notably, the effect of the filter cloth geometry on the actual food-related contamination necessitates extensive research. Morsch [19] already assumed the influence of the filter geometry and showed worse cleaning results using coarse mesh sizes.

This paper examines the time-resolved cleaning of various filter cloths with optical methods. For this purpose, a high-speed (HS) camera monitored the impact of a wash jet on a filter cloth and its cleaning effect. The cleaning efficiency and homogeneity could be deduced from these time-resolved videos. Several filter cloth types were tested, with differences in weave type, thread diameters, mesh sizes, and material. This cloth selection allowed a more thorough examination of the direct cleaning impact of common cloth properties. As model contamination, brewer's spent grains (BSG) were used to simulate a highly practice-close case study that is a frequent problem in breweries. The

findings yielded important conclusions about different cleaning phases and the effect of the cloth on its cleanability.

2 Material and Methods

2.1 Filter Cloth Types

Eleven different cloth types were selected for the experiments, varying in weave type, material, and mesh size (for the properties, see Tab. 1). The cloth manufacturers were Sefar AG (Thal, Switzerland) and Otto Markert & Sohn GmbH (Neumünster, Germany). This selection emphasized the individual impact on cleanability and covered a wide range of cloth types in this application field. Fig. 1 shows top views of the samples with the

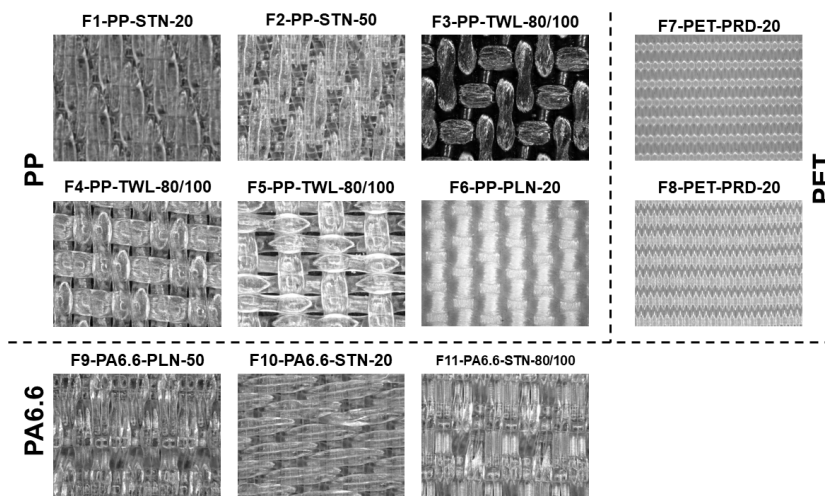


Figure 1. Top-view images of the filter cloth samples with their respective designations (magnification 20 \times), clustered according to the material.

Table 1. Filter cloth samples with specific properties and manufacturer description.^{a)}

Type	Type (mfr.) ^{a)}	Thread material	Weave pattern	Mesh sizes (mfr.) ^{a)} [μm]	Thickness (mfr.) ^{a)} [μm]	R_a [μm]	S_a [μm]
F1-PP-STN-20	05-1001-SK 020	PP	STN	20	500	4.2	16.9
F2-PP-STN-50	05-1001-K 043	PP	STN	50	540	6.3	27.6
F3-PP-TWL-80/100	05-1001-K 70 \times 320	PP	TWL	80, 100	530	3.5	13.6
F4-PP-TWL-80/100	05-1001-K 120	PP	TWL	80, 100	480	8.5	15.1
F5-PP-TWL-80/100	05-1001-K 215	PP	TWL	80, 100	480	5.8	15.6
F6-PP-PLN-20	PP 2436 (calendared)	PP	PLN (multifilament)	< 20	780	33.8	68.2
F7-PET-PRD-022	07-76-SK 022	PET	PRD	< 20	185	13.5	20.1
F8-PET-PRD-012	07-90-SK 012	PET	PRD	< 20	80	6.5	6.9
F9-PA6.6-PLN-50	03-1001-SK 066	PA6.6	PLN	50	520	6.6	21.1
F10-PA6.6-STN-20	03-1010-SK 038	PA6.6	STN	20	470	5.6	19.1
F11-PA6.6-STN-80/100	03-1001-K 080	PA6.6	STN	80, 100	520	12.3	30.2

^{a)} Information source: technical data sheet of the respective manufacturer.

surface geometry captured by a digital microscope (VHX-200D; Keyence Corporation, Osaka, Japan) with a magnification factor of 20 \times .

The woven cloths could be categorized into three clusters according to their material: polypropylene (PP), polyethylene terephthalate (PET), and polyhexamethylene adipamide (PA6.6). The mesh sizes ranged from <20 to 100 μm . The weave patterns of the samples were either plain (PLN), satin (STN), or twill (TWL). In addition, samples with a plain reverse Dutch (PRD) weave were used. This weave structure differed from the standard PLN in that the warp and weft thread diameters were different. The surface roughness was measured using a surf mobile confocal microscope (NanoFocus AG, Oberhausen, Germany) in accordance with ISO 4287 [20] and ISO 25178 [21]. The mean roughness index R_a ¹⁾ and the mean arithmetic height value S_a were selected to define the individual line and surface roughness [21]. While R_a described the roughness profile on a particular measurement line, S_a extended the measurements and specified the entire surface. The value of S_a represented the height difference between each two points and the surface arithmetic mean.

2.2 HS Camera System and Video Acquisition

The camera VW9000 and the objective VH-Z20R/Z20T (Keyence Corporation, Osaka, Japan) were used for monitoring the cleaning process. The system recorded HS videos at 500 frames per second for 2.0 s, with an exposure time of 1/1000 s. The resulting videos provided high-quality slow-motion videos that allowed tracing of the entire cleaning. Each video could be divided into single images to show the cleaning in greater detail and for further data evaluation. Any further advantages and disadvantages of the system are discussed in the Supporting Information (SI).

2.3 Cleaning Setup

The experimental studies were conducted in a cleaning device developed for the pilot filter press Meura 2001 (MEURA, Péruwelz, Belgium) in the Research Brewery Weihenstephan (Fig. 2). In this case, a traverse system allowed for an automated approach of the cleaning nozzle to the filter, resulting in a demand-oriented cleaning procedure. The applied cleaning nozzle was the full/round jet nozzle 544.360.30.CA.00.1

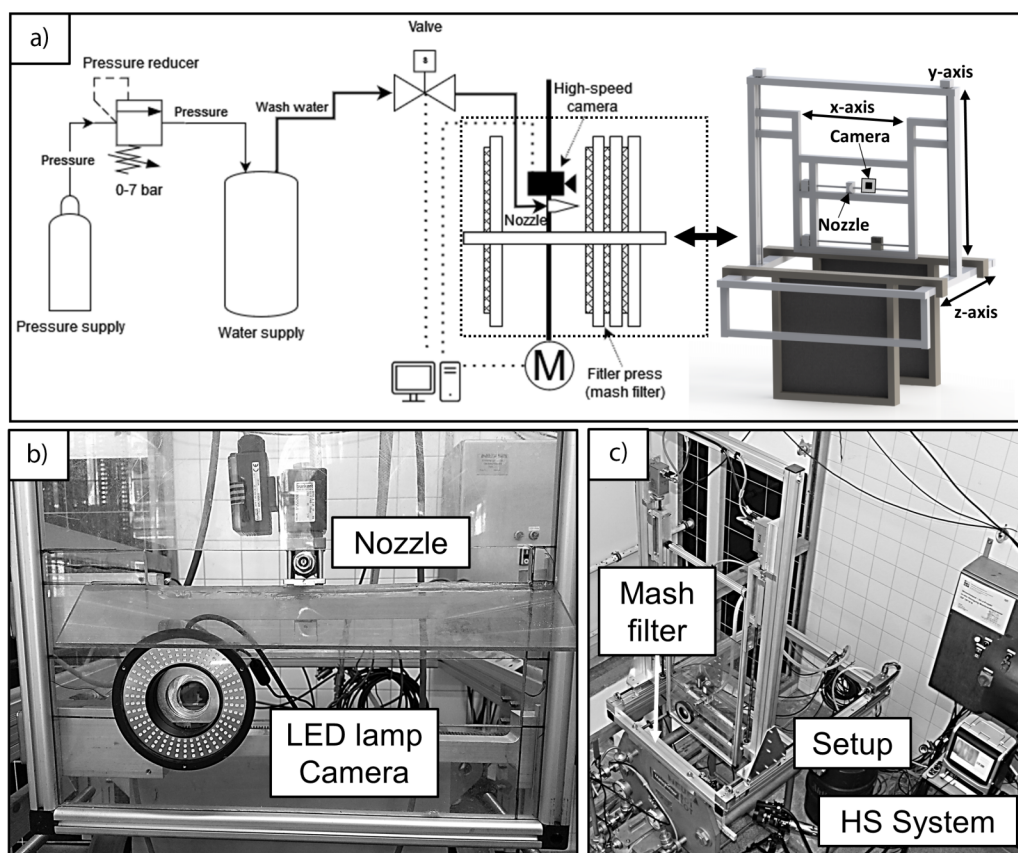


Figure 2. Experimental setup. (A) Process flow chart and computer-aided design (CAD) drawing of the setup. (B) Opto-mechanical cleaning unit. (C) Setup overview with the HS system and the mash filter.

1) List of symbols at the end of the paper.

(Lechler GmbH, Metzingen, Germany), using a pressure of 3×10^5 Pa. More details about the setup automation and the nozzle can be found in the SI.

In most experiments, the cleaning time was 2.0 s, which was long enough to see the full impact of an impacting jet on the cloth surface. According to Siekmann et al. [22] and Sigloch [23], the main effect of the cleaning occurs within the first 1.5 s, which is why the selected time frame enabled sufficient observation of the different cleaning phases. In all experiments, the distance between the cleaning nozzle and the cloth surface was 35 mm (z -axis). This value originated from previous publications of Morsch et al. [13, 14], where this distance demonstrated high suitability.

2.4 Preparation of the Contamination

For the model contamination, the industrial example brewery was selected. Thus, a practical method was necessary to produce a standardized BSG composition. According to the literature [24, 25], BSG is a complex mixture of proteins, carbohydrates, water-insoluble components (husks), and other partially sticky substances. These variables provided a good starting point for a model contaminant with adhesive and cohesive binding forces.

The preparation of this BSG-based model contamination followed the congress mash method according to MEBAK (Mitteleuropäische Brautechnische Analysenkommission) (see the SI) [26]. This practical procedure allowed the creation of a standardized fouling matrix to analyze cleaning effects in the experimental runs. The particle size distribution q_3 of the malt particles in the mash was measured with a Mastersizer 3000 (Malvern Instruments, Malvern, UK) and ranged from > 5 to $1000 \mu\text{m}$, with the most significant proportion in the range of $20\text{--}225 \mu\text{m}$. Regarding the mesh sizes (Tab. 1), these particle sizes could be retained by the cloths to deposit in the mesh apertures.

2.5 Soiling of Filter Cloths

The respective filter cloth with a total size of $297 \text{ mm} \times 210 \text{ mm}$ was clamped in a frame to simulate cloth tightening similar to that in a filter plate. Then, an acrylic glass pattern with six round holes (7 cm in diameter) was placed on the clamped cloth, generating reproducible contamination spots. Finally, 20 mL of the prepared congress mash was poured homogeneously into each pattern hole. Afterward, a specific sedimentation time of 1.5 h at 20°C was used to allow particles to penetrate the meshes, form adhesive forces to the surface, create cohesive forces and achieve a filter cake with defined moisture. The contaminated filter cloth had been placed in the cleaning apparatus and was ready for the experimental trials. The cloths were posi-

tioned vertically to simulate the condition of nozzle cleaning in a filter press.

3 Results and Discussion

3.1 Video Evaluation and Cleaning Analysis

The automated cleaning device approached each prepared contamination spot and fired a precise jet. This procedure produced a distinct cleaning effect dependent on the properties of the cloth. All other parameters, like the nozzle, the cleaning fluid, and the contamination, were kept constant.

In every case, the HS camera system captured a full video and could thus monitor the cleaning. As a result of these slow-motion videos, an analysis method was developed to identify the cleaning progress time dependently. The videos were cut into frames, resulting in single images in BMP format. Finally, only the tenth image in chronological order was used for analysis to reduce the complexity of the measurement results. Thus, a specific image processing algorithm was used to perform the final residue analysis on each image.

The acquired images were analyzed by a batch evaluation algorithm programmed using MATLAB 2019b by MathWorks® (Natick, MA, USA). The code was based on a threshold analysis and the contrast between the contamination and the filter cloth. The advantage of this method was its quick analysis combined with high precision. Any information about the detection procedure and the developed algorithm can be found in the SI. The analysis results were used to determine the cleaning degree G and the cleaning homogeneity HF of each cloth. Fig. 3 depicts the residue analysis by listing the required steps and exemplary recordings.

The parameter used to determine the cleanability was the cleaning degree G . It represented the area cleaned by the impacting jet. The cleaning degree was computed by

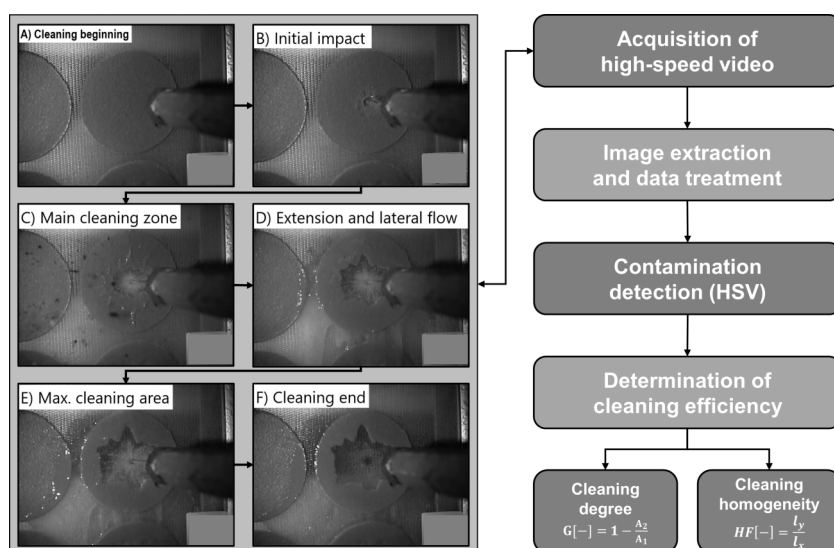


Figure 3. Schematic illustration of the image-processing procedure and determined parameters evaluating the cleaning efficiency.

comparing the contamination load in pixels before cleaning, A_1 , and after cleaning, A_2 (Eq. (1)).

$$G[-] = 1 - \frac{A_2}{A_1} \quad (1)$$

A value of 0 means no cleaning effect was observed, while 1 designated the complete residue removal.

However, G only showed the total effect on the surface without specifying any locally resolved cleaning effects. During the initial experimental runs, it became clear that each filter cloth displayed a distinct form of the cleaned surface. As a result, a location-based and appropriate cleaning pattern calculation method became necessary. For this purpose, the homogeneity factor HF as a second characteristic was introduced, illustrated in Eq. (2).

$$HF[-] = \frac{l_y}{l_x} \quad (2)$$

A process engineering approach to evaluate characteristic particle forms was adapted for the determination of HF . Here, the most extended length of the cleaned surface in y - (l_y) and x -direction (l_x) was measured with MATLAB by MathWorks® (USA) – the division of y to x results in HF . A value of 1 indicates that the cleaning effect acted homogeneously in a circular cleaning shape. Any deviation denotes a heterogeneous cleaning effect.

Fig. 4 shows the procedure for the determination of l_y and l_x and the decision criteria. The selection of l_n was based on the most extended range within the respective quadrant of the x - y coordinate system.

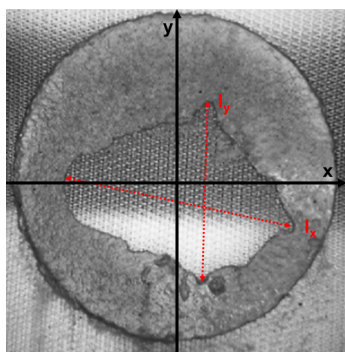


Figure 4. Exemplary cleaned filter cloth with geometric decision criteria for l_y and l_x .

3.2 Cleanability of the Selected Filter Cloth as a Function of the Cleaning Time

Fig. 5 illustrates the time-resolved cleaning degrees of the filter cloths. Since Leipert et al. [10] found only a minor material influence, the results were clustered material-dependently into three subfigures. Following Mauermann [27], cleaning time-resolved monitoring is crucial for analyzing occurring effects and efficiency.

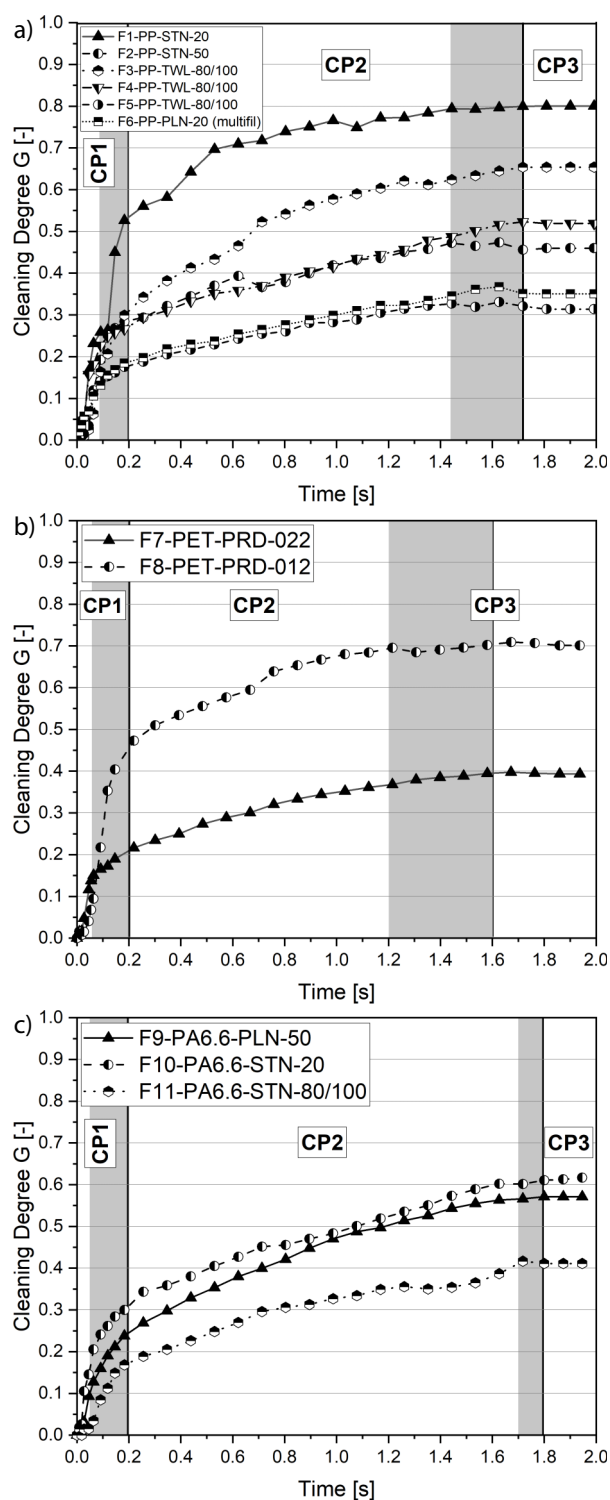


Figure 5. Gradual development of the cleaning degree G of 11 filter cloths, grouped according to the material. Cloths manufactured of (A) PP, (B) PET, (C) PA6.6. CP = cleaning phase (individual sections are qualitatively visualized using a gray-colored area). Other constant cleaning parameters: $v = 11.44 \text{ m s}^{-1}$, $p = 3 \times 10^5 \text{ Pa}$, $X_{\text{Nozzle_Surface}} = 35 \text{ mm}$, $T = 22^\circ\text{C}$, $n = 6$. The confidence intervals ($\alpha = 0.05$) ranged from 0.05 to 0.10 and are not shown in the graph for readability.

The results showed increasing cleaning degrees over time. In most cases, the curves followed different cleaning efficiencies, resulting in different final cleaning degrees G . However, in no case did the filter cloths reach a G value of 1.0. This can be attributed to the fact that the contaminated area was selected as oversized. This size was used in all experiments as the specific area to be cleaned was the decisive criterion. So, it was unimportant whether the specific cleaning concept also cleaned the entire experimental surface. Therefore, this overdimensioning even turned out to be an advantage, as it enabled a high degree of comparability between the different cleaning experiments. As a result, different cleaning effects could occur within the same material cluster, implying that a material influence could not be demonstrated. This aspect was remarkable as the material specifically influences the cleaning surfaces. Here, the surface energy or wettability (e.g., determination via contact angles) is essential to consider [8]. However, concerning filter cloths, the complex structured surfaces seem to have more influence on the cleanability.

Initially, the contamination was homogeneous in each spot, and the effecting cleaning parameters were kept constant. As a result, the cleaning success had to depend on the filter structure, such as different weaves, meshes, and thread sizes. Individual properties (Tab. 1) revealed higher G in cleaning cloths with smaller mesh sizes, indicating better cleanability. Significantly, this aspect was represented by F1-PP-STN-20, F8-PET-PRD-012, and F10-PA6.6-STN-20, which showed the best cleanability while having the smallest meshes. The coarser meshes almost always resulted in the lowest cleaning degree. This observation could be combined with the findings of the roughness profiles in Tab. 1. For instance, all filters with the best cleanability also have minor R_a and, in parts, S_a values.

Furthermore, the weave type, as an additional central parameter, had an effect that was directly related to the mesh size and thread diameter. When the mesh sizes were small, PLN and STN weaves favored cleanability. The weave pattern explained this observation where the PLN and STN weaves show more homogeneous structures than TWL. These parameters were also part of other research findings in which smooth surfaces showed an appropriate hygienic design. Consequently, a significant influence of the filter geometry on the cleanability could be concluded.

The multiple yarn, which resulted in poor cleanability, was an exception to these findings. The previous conclusion could be underlined as the filter cloth F6-PP-PLN-20 showed the highest R_a and S_a values due to the increased roughness. This yarn bunch is also thicker, resulting in deeper valleys between the threads. At first glance, this conclusion contradicts the findings of Morsch et al. [13], who found multifil weaves more easily cleanable. However, these results were based on cleaning in a small area; so, a detailed observation of the cleaning phases was still required. The entire contamination was located in the impact area where most of the forces of the initial jet could have an effect (Fig. 6C).

The overall cleaning progress resulted in distinct phases that allowed for cloth-specific cleaning classification. The respective end times are illustrated in the SI. Cleaning phase 1 could be observed at the beginning, where the central cleaning zone formed. All cleaning curves show the same cleaning progress, with the zone (impact area) expanding to a cloth-specific maximum. This zone was visible in the related videos as white flow zones on the cloth in the jet impact area. Wilson et al. [28] demonstrated that this area could be equalized to the radial flow zone (RFZ) for flat solid surfaces (Fig. 6). Initially, shock waves and, later, lateral flows acted on the surrounding area, and the jet generated enough pressure to clean all filter cloths uniformly. The impacting fluids underwent dynamic compression, decelerating until almost zero velocity [23,27]. This impact force caused a shock wave (also water hammer) against the fluid jet and into the contamination, which created the initial strong cleaning effect by bursting the top layer. Arising forces overcame the cohesive forces within the contamination and also adhesive forces of the contamination towards the cloth surface in the impact area. Subsequently, the jet could penetrate the contamination down to the filter cloth, forming the RFZ. Flows streamed laterally to all sides from the point of impact, which removed the surrounding contamination and resulted in phase 2.

In phase 2, the cleaning degrees diverged significantly in most cases. Here, fluid friction and reduced wall shear stress along the surface reduce cleaning. Because of the cohesive and robust interaction effect of the filter cake, the removal was further downgraded. Any cleaning flow influence required sufficient pressure and wall shear stress along the surface to

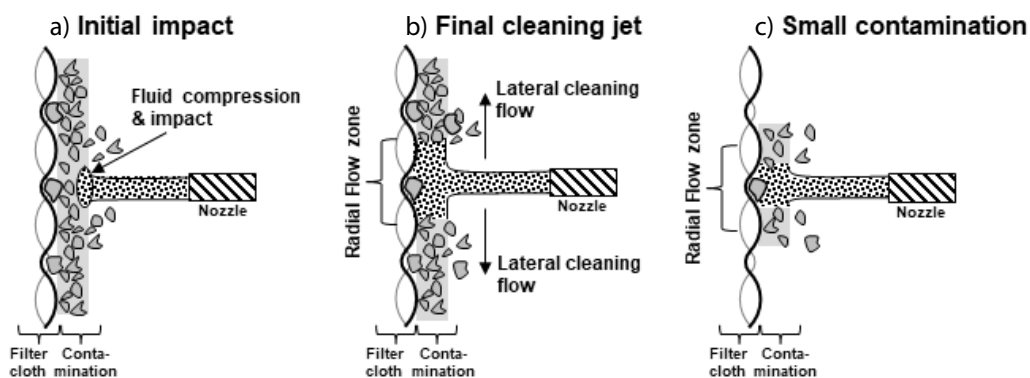


Figure 6. Schematic illustration of the jet (A) at initial impact, (B) in its final shape, and (C) at a small contaminated area.

overcome the acting adhesive forces. However, the cleaning effect differed between the filter cloth types in phase 2. It had to be concluded that the different cleanability had to depend on the filter geometry as well. After approximately 1.4–1.6 s (PP, PET) and 1.8 s (PA6.6), the cleaning progress followed an asymptotic trend, turning into constant G values. Here, the final cleaning phase 3 was reached, and no further cleaning took place. The highest pressure forces were observed in the impact area of the wash jet during cleaning phase 1, accomplishing cleaning with the highest reliability and performance here.

3.3 Cleaning Homogeneity at Selected Cleaning Times

So far, a significant influence of the filter geometry on the cleanability of a cloth has been determined. Significantly, the combination of mesh sizes and weave type, as well as the resulting roughness profile, could be identified as essential. The previous results, however, did not determine the location-specific cleaning effects. Another study [17] discovered an impact in areas other than the RFZ. However, it was unclear how uniformly the cleaning effect decreased away from the RFZ. For these reasons, the HF homogeneity factor was created. This parameter was monitored for all applied filters in equal material clusters. Fig. 7 displays the time-resolved results of the experimental investigations.

The results of HF represented the homogeneity of the cleaning effect. Values near $HF = 1$ demonstrated a circular cleaning effect in the range, indicating a homogeneous cleaning. Respective values above 1 and higher displayed a more considerable cleaning effect in the y -direction, while a score below 1 and lower represented more cleaning influence in the x -coordinate. It can be hypothesized that the lateral flow direction of the impinging jet is associated with a particular deflection potential of the filter cloth.

First, in all diagrams, equal curves could be observed. During cleaning phase 1, all filter cloths showed values of HF around 1, which evidenced a very homogeneous cleaning effect. The corresponding cloth areas only covered a small portion of the contaminated area. In cleaning phase 2, a split between several cloths could be noticed. HF remained constant until cleaning phase 3 was reached. This observation demonstrated that the wash water distribution on the cloth is consistent. The contamination outside the RFZ was constantly removed, depending on the cloth parameters. However, the weave type had to be taken into account, particularly in terms of filter geometry. Because of the homogeneous cloth structure, the PLN with monofil threads was cleaned homogeneously. It was followed by STN, which produced reliable homogeneity in almost all cases. More heterogeneous results were observed when a TWL or a PRD weave was applied. This was due to the typical weave structures of the woven cloths, as illustrated in Fig. 8. The structures and resulting geometries of these weave patterns could be assumed to create flow. The fluid-dynamical obstacles resulted in an inhomogeneously cleaned area that only improved drainage in specific directions. In addition to the adhesive and cohesive forces, the contamination that adhered to the deeper cloth

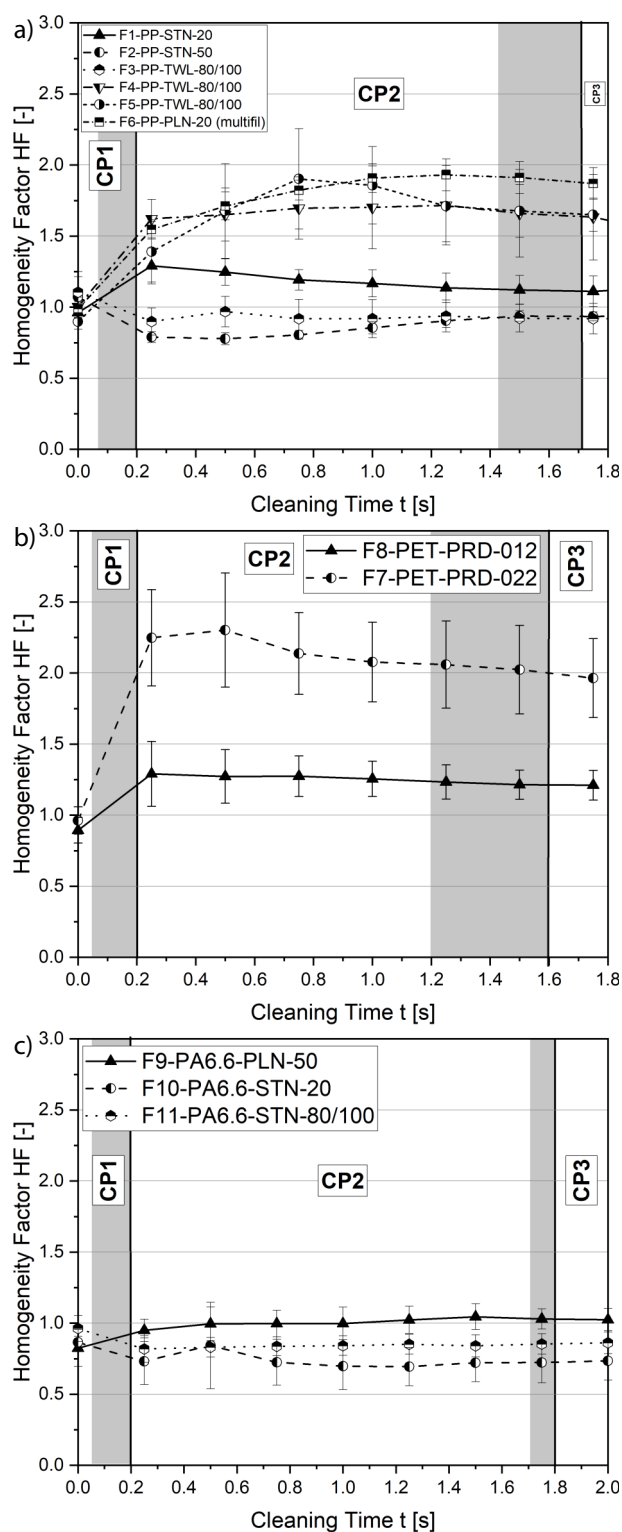


Figure 7. Homogeneity factors depending on the cleaning time. Values close to $HF = 1$ designate homogeneous cleaning areas; any deviations indicate heterogeneous cleaning. Cloths manufactured of (A) PP, (B) PET, (C) PA6.6. Other constant cleaning parameters: $v = 11.44 \text{ m s}^{-1}$, $p = 3 \times 10^5 \text{ Pa}$, $x_{\text{Nozzle_Surface}} = 35 \text{ mm}$, $T = 22 \text{ }^\circ\text{C}$, $n = 6$.

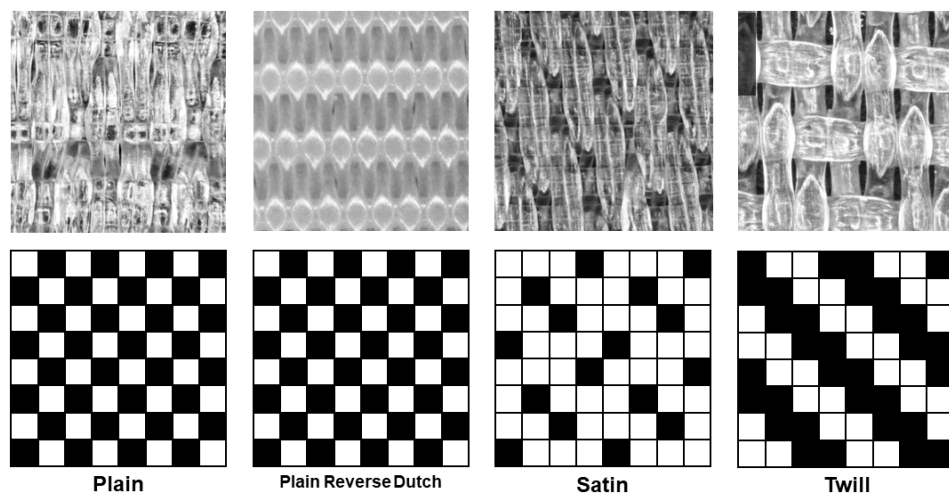


Figure 8. Weave types of the applied woven filters with schematic weave patterns to identify the flow stream. Black squares represent peaks and white squares represent the weave valleys. Illustration inspired by Purchas [29] and Anlauf [6].

layers required additional jet force to be transported out of the cloth weave valleys. Here, it is more efficient for particles and the wash stream to follow the weave-specific flow channel, resulting in a higher deviation of HF . During the stream away from the RFZ, the fluid friction increased, resulting in declined G and HF .

Additionally, two additional exceptions required detailed analysis. First, it had to be discussed why F3-PP-TWL-80/100 resulted in a considerably better and more homogeneous cleanability than the other TWL fabrics. This cloth type, like the others, had similar properties. However, the mesh distribution and permeability were different, resulting in a more open surface finish and destructured TWL.

Second, F7-PET-PRD-022 and F8-PET-PRD-012 differed significantly in their cleanability, although PRD was applied in both cases. The solution could be found in the filter thickness. Both types were the thinnest applied types, while F8-PET-PRD-012 was even 57 % thinner. This aspect resulted in pressing of the thin cloth at the initial impact, explaining more heterogeneous cleaning and poor cleaning results, as shown in Fig. 6B. All other cloths were thicker, giving them a more resistant stiffness. So, thin filters require extra care.

4 Conclusion

The influence of the woven cloth properties on their cleanability was investigated in this experimental study using jets. HS videos were recorded with an HS camera, allowing for precise and time-resolved cleaning analysis. The results were applied using BSG, which continues to cause complex cleaning procedures in breweries.

First, the cleaning videos showed that the cleaning of filter cloths could be distinguished into three cleaning phases. Cleaning phase 1 represented the impact area, where the most intense fluid forces allowed consistent contamination removal. The properties of the filter cloth had less effect on the cleanability here. In contrast, due to friction and decreased wall

shear stress, phase 2 demonstrated decreased cleaning efficiency that was highly dependent on the woven filter type. These findings were essential as this phase comprised the longest cleaning part and the most extensive surface range. The last phase 3, illustrated a status quo where the maximum effect was reached, and no further cleaning took place.

Second, the influence of the filter geometry and its respective components on the cleanability could be detailed. The cleaning degree G and the homogeneity factor HF were used to illustrate the influencing effects primarily in cleaning phase 2. The results revealed a dependence on the filter roughness, as indicated by R_a and S_a . However, the roughness was caused primarily by the mesh sizes in combination with the weave type, which is why these factors required careful consideration. As a result, according to common hygienic design principles, rough surfaces of filter cloths will always result in complicated cleaning. In future research, these findings can be further detailed with a study concerning wettability and the surface energy of the cloth.

The presented research results help find the requirements for cleaning concepts for woven filter cloths. The weave types and mesh sizes were the most important criteria for effective and uniform cleaning. Furthermore, the findings can help to develop hygienic design guidelines. The image-based residue detection and the developed cleaning setup are suitable for improving filter presses. Automated and digitalized cleaning, in particular, can potentially be critical elements in this field [30].

Supporting Information

Supporting Information for this article can be found under DOI: <https://doi.org/10.1002/ceat.202200468>.

Data Availability Statement

The data that support the findings of this study are available from the corresponding author upon reasonable request.

Acknowledgment

This IGF Project 19716 N of the IVLV (Industrievereinigung für Lebensmitteltechnologie und Verpackung e.V., Freising, Germany) is supported via AiF within the program for promoting the Industrial Collective Research (IGF) of the German Ministry of Economic Affairs and Energy (BMWi), based on a resolution of the German Parliament. Open access funding enabled and organized by Projekt DEAL.

The authors have declared no conflict of interest.

Symbols used

A_n	[m ²]	surface
G	[-]	cleaning degree
HF	[-]	cleaning homogeneity factor
l_n	[m]	length
R_a	[μm]	mean roughness index
S_a	[μm]	mean arithmetic height value

Abbreviations

BSG	brewer's spent grains
HS	high-speed
PA6.6	polyhexamethylene adipamide
PET	polyethylene terephthalate
PLN	plain
PP	polypropylene
PRD	plain reverse Dutch
RFZ	radial flow zone
STN	satın
TWL	twill

References

- [1] DIN 10516, *Lebensmittelhygiene – Reinigung und Desinfektion*, Beuth, Berlin **2020**.
- [2] G. Wildbrett, *Reinigung und Desinfektion in der Lebensmittelindustrie*, 2nd ed., Behr, Hamburg **2006**.
- [3] J. Hofman, Stoffübergang bei der Reinigung als Qualifizierungsmethode der Reinigbarkeit, *Ph.D. Thesis*, Technical University of Munich, Freising-Weihenstephan **2007**.
- [4] H. Stoye, H. Köhler, M. Mauermann, J.-P. Majschak, *Chem. Ing. Tech.* **2014**, 86 (5), 707–713. DOI: <https://doi.org/10.1002/cite.201300047>
- [5] H. Köhler, H. Stoye, M. Mauermann, T. Weyrauch, J.-P. Majschak, *Food Bioprod. Process.* **2015**, 93, 327–332. DOI: <https://doi.org/10.1016/j.fbp.2014.09.010>
- [6] H. Anlauf, *Wet Cake Filtration: Fundamentals, Equipment, and Strategies*, 1st ed., Wiley-VCH, Weinheim **2019**.
- [7] *DOC 8: Hygienic Design Principles*, 3rd ed., European Hygienic Engineering & Design Group, Frankfurt **2018**.
- [8] M. Mauermann, J.-P. Majschak, T. Bley, C. Bellmann, A. Calvimontes, A. Caspari, *Chem. Ing. Tech.* **2012**, 84 (9), 1568–1574. DOI: <https://doi.org/10.1002/cite.201100232>
- [9] R.-S. Möller, Haftkräfte, Alterung und Überwachung funktionaler Oberflächen – Gärtücher im Gebrauch, *Ph.D. Thesis*, Karlsruhe Institute of Technology **2018**.
- [10] C. Leipert, H. Nirschl, *Filtr. Sep.* **2011**, 25 (5), 270–277.
- [11] S. Stahl, S. Siggelkow, H. Nirschl, *Eng. Life Sci.* **2007**, 7 (2), 136–142. DOI: <https://doi.org/10.1002/elsc.200620183>
- [12] S. Stahl, C. Leipert, H. Nirschl, *Sep. Purif. Technol.* **2013**, 110, 196–201. DOI: <https://doi.org/10.1016/j.seppur.2013.02.003>
- [13] P. Morsch, J. Kühn, R. Werner, H. Anlauf, D. U. Geier, T. Becker, H. Nirschl, *Chem. Eng. Sci.* **2020**, 226, 115889. DOI: <https://doi.org/10.1016/j.ces.2020.115889>
- [14] P. Morsch, A. Arnold, H. Schulze, R. Werner, H. Anlauf, D. U. Geier, T. Becker, H. Nirschl, *Sep. Purif. Technol.* **2021**, 256, 117793. DOI: <https://doi.org/10.1016/j.seppur.2020.117793>
- [15] C. Weidemann, Reinigungsfähigkeit mithilfe kontinuierlicher und pulsierender Strömung, *Ph.D. Thesis*, Karlsruhe Institute of Technology **2014**.
- [16] C. Weidemann, S. Vogt, H. Nirschl, *J. Food Eng.* **2014**, 132, 29–38. DOI: <https://doi.org/10.1016/j.jfoodeng.2014.02.005>
- [17] R. Werner, B. Bollwein, R. Petersen, J. Tippmann, T. Becker, *Chem. Eng. Technol.* **2017**, 40 (3), 450–458. DOI: <https://doi.org/10.1002/ceat.201600049>
- [18] C. Leipert, H. Nirschl, *Chem. Ing. Tech.* **2012**, 84 (8), 1285. DOI: <https://doi.org/10.1002/cite.201250370>
- [19] P. Morsch, Detachment of fine-grained thin particle layers from filter media, *Ph.D. Thesis*, Karlsruhe Institute of Technology **2021**.
- [20] DIN EN ISO 4287, *Geometrical Product Specifications (GPS) – Surface texture: Profile method – Terms, definitions and surface texture parameters*, Beuth, Berlin **2010**.
- [21] DIN EN ISO 25178-2, *Geometrical Product Specifications (GPS) – Surface texture: Areal – Part 2: Terms, definitions and surface texture parameters*, Beuth, Berlin **2020**.
- [22] H. E. Siekmann, P. U. Thamsen, *Strömungslehre für den Maschinenbau: Technik und Beispiele*, 2nd ed., Springer, Berlin **2009**.
- [23] H. Sigloch, *Technische Fluidmechanik*, 10th ed., Springer, Berlin **2017**.
- [24] M. Santos, J. Jiménez, B. Bartolomé, C. Gómez-Cordovés, M. Del Nozal, *Food Chem.* **2003**, 80 (1), 17–21. DOI: [https://doi.org/10.1016/S0308-8146\(02\)00229-7](https://doi.org/10.1016/S0308-8146(02)00229-7)
- [25] J. Steiner, S. Procopio, T. Becker, *Eur. Food Res. Technol.* **2015**, 241 (3), 303–315. DOI: <https://doi.org/10.1007/s00217-015-2461-7>
- [26] *MEBAK brautechnische Analysenmethoden – Rohstoffe. Rohfrucht, Gerste, Malz, Hopfen und Hopfenprodukte: Methodensammlung der Mitteleuropäischen Brautechnischen Analysenkommission* (Ed: F. Jacob), Selbstverlag der MEBAK, Freising-Weihenstephan **2016**.
- [27] M. Mauermann, Reinigbarkeit von Oberflächen in der Lebensmittelindustrie durch Flüssigkeitsstrahlen, *Ph.D. Thesis*, Technische Universität Dresden **2012**.
- [28] D. I. Wilson, B. L. Le, H. Dao, K. Y. Lai, K. R. Morison, J. F. Davidson, *Chem. Eng. Sci.* **2012**, 68 (1), 449–460. DOI: <https://doi.org/10.1016/j.ces.2011.10.003>
- [29] D. B. Purchas, K. Sutherland, *Handbook of Filter Media*, 2nd ed., Elsevier, Oxford **2002**.
- [30] M. Windisch, V. Seifert, M. Mauermann, *Adhaes. – Kleben Dichten* **2018**, 62 (11), 26–29. DOI: <https://doi.org/10.1007/s35145-018-0076-4>